Characteristics of root pullout resistance of *Caragana korshinskii* Kom. in the loess area of northeastern Qinghai-Tibet Plateau, China

LIU Yabin[1,2*], SHI Chuan[1], YU Dongmei[3,4], WANG Shu[1], PANG Jinghao[1], ZHU Haili[1,2], LI Guorong[1,2], HU Xiasong[1,2*]

[1] Department of Geological Engineering, Qinghai University, Xining 810016, China;
[2] Key Laboratory of Genozoic Resource & Environment in North Margin of the Tibetan Plateau, Xining 810016, China;
[3] Key Laboratory of Comprehensive and Highly Efficient Utilization of Salt Lake Resources, Qinghai Institute of Salt Lakes, Chinese Academy of Sciences, Xining 810008, China;
[4] Qinghai Provincial Key Laboratory of Geology and Environment of Salt Lakes, Xining 810008, China

Abstract: Roots exert pullout resistance under pullout force, allowing plants to resist uprooting. However, the pullout resistance characteristics of taproot-type shrub species of different ages remain unclear. In this study, in order to improve our knowledge of pullout resistance characteristics of taproot systems of shrub species, we selected the shrub species *Caragana korshinskii* Kom. in different growth periods as the research plant and conducted *in situ* root pullout test. The relationships among the maximum pullout resistance, peak root displacement, shrub growth period, and aboveground growth indices (plant height and plant crown breadth) were analyzed, as well as the mechanical process of uprooting. Pullout resistance of 4–15 year-old *C. korshinskii* ranged from 2.49 (±0.25) to 14.71 (±4.96) kN, and the peak displacement ranged from 11.77 (±8.61) to 26.50 (±16.09) cm. The maximum pullout resistance and the peak displacement of roots increased as a power function (R^2=0.9038) and a linear function (R^2=0.8242) with increasing age, respectively. The maximum pullout resistance and the peak displacement increased with increasing plant height; however, this relationship was not significant. The maximum pullout resistance increased exponentially (R^2=0.5522) as the crown breadth increased. There was no significant relationship between the peak displacement and crown breadth. The pullout resistance and displacement curve were divided into three stages: the initial nonlinear growth, linear growth, and nonlinear stages. Two modes of failure of a single root occurred when the roots were subjected to vertical loading forces: the synchronous breakage mode and the periderm preferential breakage mode. These findings provide a foundation for further investigation of the soil reinforcement and slope protection mechanisms of this shrub species in the loess area of northeastern Qinghai-Tibet Plateau, China.

Keywords: loess area; Qinghai-Tibet Plateau; pullout resistance; growth period; aboveground growth indices; pullout test; *Caragana korshinskii*

Citation: LIU Yabin, SHI Chuan, YU Dongmei, WANG Shu, PANG Jinghao, ZHU Haili, LI Guorong, HU Xiasong. 2022. Characteristics of root pullout resistance of *Caragana korshinskii* Kom. in the loess area of northeastern Qinghai-Tibet Plateau, China. Journal of Arid Land, 14(7): 811–823. https://doi.org/10.1007/s40333-022-0023-y

1 Introduction

When plants are subjected to external loading forces on their surfaces, such as runoff and wind, or

*Corresponding authors: LIU Yabin (E-mail: liuyabincug@163.com); HU Xiasong (E-mail: huxiasong@sina.com)
Received 2022-03-30; revised 2022-06-17; accepted 2022-06-29

landslide loads, the roots below the ground or sliding surfaces must withstand pullout force. Under pullout force, the root-soil interactions result in pullout resistance, which ensures that the plant can withstand uprooting by external loading forces, and provides an anchoring effect in shallow slope soil (Wu et al., 1979; Waldron and Dakessian, 1981; Crook and Ennos, 1996; Stokes et al., 2009; Schwarz et al., 2011). Therefore, according to the characteristics of pullout resistance of plant roots, researchers assessed the windbreak and sand fixation abilities of plants, as well as their effects on water and soil conservation, and slope protection (Stokes et al., 1996; Norris, 2005; van Beek et al., 2005; Stubbs et al., 2019).

The characteristics of pullout resistance of plant roots include both the root pullout resistance and its influencing factors. Numerous studies have obtained the pullout resistance of roots of different plants via pullout test. Researchers have studied the effects of many pullout resistance influencing factors, including the type of root system, the root morphological indices, the aboveground growth indices, the tensile mechanical properties of a single root, the plant growth period, and the physical and mechanical properties of soils based on pullout test and numerical simulations (Mickovski and Ennos, 2003; Dupuy et al., 2005; Burylo et al., 2009; Stokes et al., 2009; Tian et al., 2014).

The type of root system is a key factor influencing the characteristics of plant root pullout resistance (Stokes et al., 1996; Ali et al., 2013). Tree roots have been classified into three main types: tap, heart, and flat roots (Köstler et al., 1968). Plants possessing heart and taproot systems are the most resistant to uprooting (Dupuy et al., 2005; Stokes et al., 2009), especially the vertical taproot (Yang et al., 2017; Yang et al., 2018). In addition, the branching angle between lateral roots and taproot also affects the characteristics of pullout resistance of taproot system (Fourcaud et al., 2008; Ali et al., 2013). The root morphological indices include the total surface area, total volume, total length, dry weight, and the number of lateral roots (Dupuy et al., 2005; Yang et al., 2021). For different types of plant roots, these root morphological indices are positively correlated with root pullout resistance. Especially, the root surface area is better than other indices for reflecting pullout resistance (Yang et al., 2021). In addition, the aboveground growth indices, such as plant height, diameter at breast height, stem basal diameter, and crown biomass are important traits related to root pullout resistance (Cucchi et al., 2004; Burylo et al., 2009). The tensile mechanical properties of a single root include single root tensile force, single root tensile strength, single root limit extensile rate, root elastic modulus, and root stiffness are also key factors influencing root pullout resistance (Genet et al., 2005; Mickovski et al., 2007; Boldrin et al., 2017; Zhang et al., 2019). And the tensile mechanical properties are intrinsic factors that determine the deformation and failure of roots when subjected to pullout forces (Wu et al., 1979; Mickovski et al., 2007; Schwarz et al., 2011).

Plant roots grow continuously, resulting in an obvious temporal effect on plant uprooting. Thus, the characteristics of pullout resistance of plant roots are dynamic (Scippa et al., 2006; Stokes et al., 2009). Zhang et al. (2012) conducted *in situ* pullout test to assess the pullout resistance of four shrubs with growth periods of 1–4 a in the Xining Basin, China. Their results revealed that the root pullout resistance of the four shrub species increased as a power function, a linear function, and an exponential function with an increasing growth period. The root pullout resistance was also influenced by the soil physical and mechanical properties, such as soil moisture content, density, and shear strength (Mickovski et al., 2007; Zhang et al., 2020). Affected by root types, the relationship between root pullout resistance and soil moisture content is variable; for example, studies have found that root pullout resistance initially increased with soil moisture content, and then decreased (Wang et al., 2017), or root pullout resistance decreased linearly as soil moisture content increased (Schwarz et al., 2011; Zhang et al., 2020). The greater the soil density, the greater the shear strength of root-soil interface, which results in an increase in root pullout resistance (Su et al., 2020). When plant roots are uprooted, the soil around the roots will resist the shear stress; hence, the soil shear strength directly affects the stability of root-soil interface (Ennos, 1989; Zhou et al., 1998).

The root material and soil matrix are elastic-plastic materials. When roots are subjected to

uprooting, the transmission of force between roots and soil is a complex nonlinear process (Ennos, 1989; Norris, 2005). Previous studies have investigated the pullout behaviors of roots being pulled out through analyzing root pullout resistance and displacement curves with pullout test (Ennos, 1989; Ennos, 1990; Bailey et al., 2002; Mickovski et al., 2005; Mickovski et al., 2007; Schwarz et al., 2011; Tian et al., 2014; Su et al., 2020). The characteristics of mechanical process and failure mode of the roots being pulled out can be determined by displacement curves.

Although studies have investigated the characteristics of root pullout resistance, the relationship between root pullout resistance and plant growth period, especially for shrub species with longer growth periods is less concerned. In addition, there are few reports on the root pullout resistance of perennial shrub species in the loess area of northeastern Qinghai-Tibet Plateau, China. The objectives of this study were: (1) to determine the relationship between root pullout resistance and plant growth period; (2) to investigate the relationship between root pullout resistance and aboveground plant growth indices, including plant height and plant crown breadth; and (3) to analyze the mechanical process and failure modes by which taproot-type shrub species resist uprooting. The results of this study would provide a foundation for further investigation of soil reinforcement and slope protection by shrub species in the loess area.

2 Materials and methods

2.1 Study site

Northeastern Qinghai-Tibet Plateau is located at the intersection between sub-humid temperate continental monsoon climate zone, inland arid zone, and the high-cold area in eastern China. Loess is widely distributed and characterized by high sediment thickness and relatively complete strata. The Xining Basin and its surrounding areas are the main loess sedimentary area in northeastern Qinghai-Tibet Plateau (Tan et al., 2006). Due to the neotectonic movement, the loess in this area has been strongly eroded and cut, resulting in the extensive development of gullies and a landscape characterized by ridges, shoulders, tablelands, and loess hills (Zhuang et al., 2016). Most of precipitation in the Xining Basin occurs in the form of rainstorms and showers, which are characterized by short durations and high intensities (Liu et al., 2021). The slopes in this area are characterized by large gradients and low vegetation coverage, so the rainfall infiltration depth is relatively shallow, which has led to the frequent occurrence of shallow landslides, debris flows, soil erosion, and other geological disasters in the study area (Hu et al., 2013; Zhuang et al., 2016).

A site located in the Dayou Mountains in the northern Xining City, Qinghai Province, China was selected as the study area (Fig. 1a). The study site had a slope gradient of 24 °–43 ° with a northeast-facing orientation and 2350–2450 m a.s.l. elevation. The main vegetation includes shrub *C. korshinskii* and other natural herb species. *C. korshinskii* were artificially sown in 2001 (Fig. 1b). The soil physical properties are summarized in Table 1.

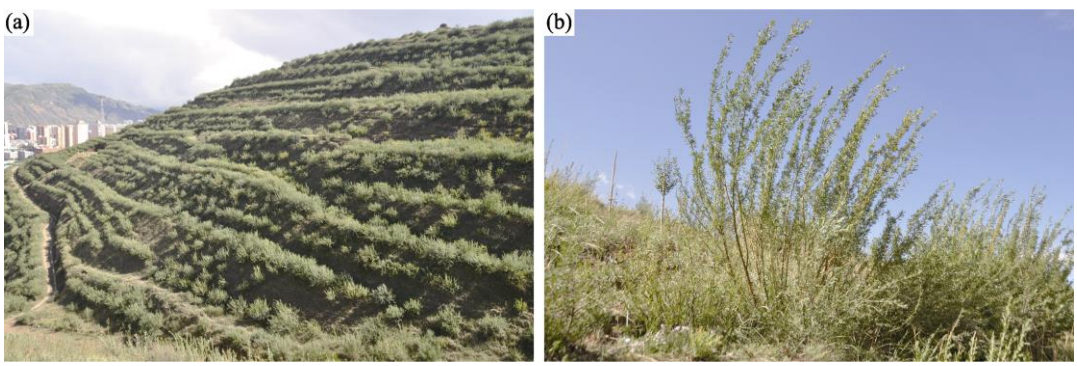

Fig. 1 (a), study site in the Dayou Mountains in the northern Xining City, China; (b), *Caragana korshinskii.*

Table 1 Soil physical properties in the study site

Depth (cm)	Dry density (g/cm^3)	Moisture content (%)	Liquid limit (%)	Plastic limit (%)	Grain composition (%)			Non-uniform coefficient	Soil type
					0.250–0.075 mm	0.075–0.005 mm	<0.005 mm		
0–30	1.28±0.10	18.61±4.10	24.08±0.66	17.34±0.38	35.16±16.04	61.88±14.76	2.97±2.12	4.73±2.58	Silt

Note: Soil moisture content and dry density are the averages around the roots in the 0–30 cm depth with 42 samples obtained for each parameter. Twelve samples were randomly selected from the study site to measure the liquid limit, plastic limit, grain composition, and non-uniform coefficient. Mean±S.D.

2.2 Plant properties

C. korshinskii is a perennial shrub species that is widely distributed on northeastern Qinghai-Tibet Plateau. *C. korshinskii* has taproot-type roots that consist of a deep taproot and many lateral roots (Niu et al., 2003). *C. korshinskii* is highly adaptable and is resistant to cold and drought, which is ideal for soil and water conservation, and slope stabilization in cold and arid regions (Hu et al., 2013; Liu et al., 2021).

2.3 *In situ* pull out test

Intact *C. korshinskii* plants were randomly selected. The slope gradient of the selected plant growth position was 24 °–30 °. A self-constructed instrument was used for *in situ* pullout test. The instrument was composed of a triangular bracket, a hand chain hoist, a clamp, a tension sensor (measurement range of 30 kN and accuracy of 0.5%), a guyed displacement sensor (measurement range of 100 cm and accuracy of 0.5%), a data acquisition system, a laptop, and batteries. *In situ* pullout test instrument is displayed in Figure 2.

Prior to *in situ* pullout test, plant height and plant crown breadth of each selected plant were measured using a steel ruler, and plant growth period was determined from annual rings in the stem. After this, plant stems and leaves were cut off, *in situ* pullout test instrument was assembled, and clamp was attached to the plant stem just above the ground surface. Before *in situ* pullout test was conducted, hand chain hoist was stretched tightly, and it was maintained on the same plumb line with plant stem, but plant roots were not subjected to tension. At the same time,

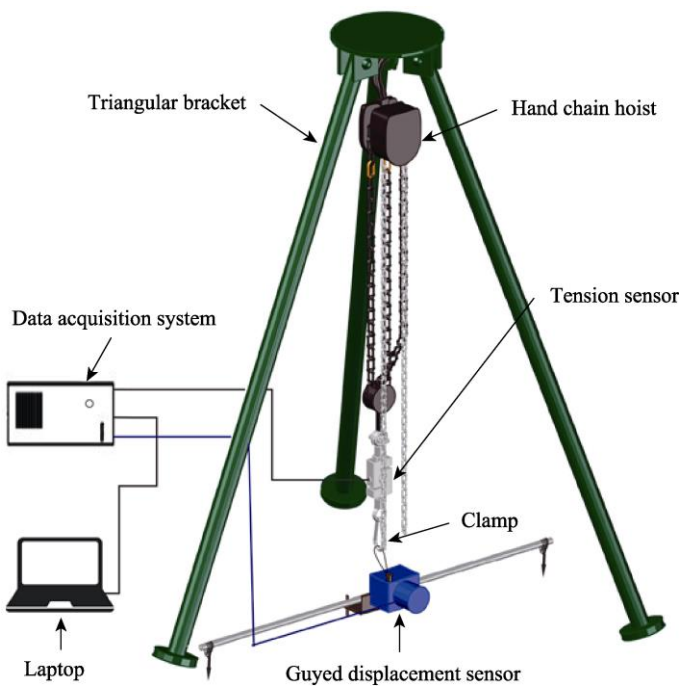

Fig. 2 Schematic diagram of the instrument for *in situ* pullout test

software on the laptop was used to initialize tension sensor and guyed displacement sensor, and begin the data acquisition system. Then, the chain was manually operated at a constant speed of 20 cm/min (average pullout rate, 21.50 (±3.71) cm/min) until root pullout resistance exceeded the peak value, and no further interaction occurred between roots and surrounding soils. Data acquisition system continuously collected pullout resistance and displacement of plant roots with an acquisition rate of 50 times per second, and these data were displayed on the software page of laptop terminal. After the test, software saved the test data automatically. In this study, a total of 42 *C. korshinskii* plants were selected for *in situ* pullout test. These plants had growth periods of 4, 5, 6, 7, 9, 12, and 15 a. Sample numbers and aboveground growth indices of these plant species are summarized in Table 2.

Table 2 Sample numbers and aboveground growth indices of *C. korshinskii*

Age (a)	Plant height (cm)	Plant crown breadth (cm)	Sample number
4	236.00±36.11^{b}	223.50±35.52^{c}	5
5	235.00±47.64^{b}	211.50±5.83^{c}	5
6	237.10±29.01^{b}	232.14±34.32^{c}	7
7	269.17±72.88^{ab}	260.00±23.76^{bc}	6
9	281.33±34.09^{ab}	273.75±28.05^{b}	6
12	304.40±34.46^{a}	280.50±21.30^{ab}	5
15	321.75±46.88^{a}	309.69±30.88^{a}	8

Note: Different lowercase letters within the same column indicate significant differences among different plant ages at $P<0.05$ level. Mean±SD.

In situ pullout test was conducted from 31 August, 2021 to 7 September, 2021. There was light rain (24 h rainfall, less than 10 mm) on 5 September, 2021, and the weather was sunny and cloudy on other days. Rainfall infiltration depth of this type of rainfall in the loess area is less than 30 cm (Wang et al., 2021). In order to avoid rainfall infiltration affecting the test results, we measured soil moisture content with the depth of 0–30 cm around the roots before and after rainfall. The test could be continued when there was no significant difference between soil moisture contents around plant roots after and before rainfall. Thus, no tests were carried out from 5 September to the afternoon of 6 September.

2.4 Statistical analysis

Regression analysis was conducted to determine the relationships of the maximum root pullout resistance and the peak displacement (the displacement corresponding to the maximum pullout resistance) with growth period of *C. korshinskii*. Regression analysis and correlation analysis also revealed the relationships of the maximum root pullout resistance and the peak displacement with plant height and plant crown breadth. Classification of correlation coefficients and correlation strengths are shown in Table 3 (Xie et al., 2013). All of the statistical analyses were performed using the Origin v.8.0 software.

Table 3 Classification of correlation strength during correlation analysis

$\|r\|<0.3$	$0.3\leq\|r\|\leq0.5$	$0.5\leq\|r\|\leq0.8$	$\|r\|\geq0.8$
Weak correlation	Low correlation	Moderate correlation	High correlation

3 Results

3.1 Relationship between root pullout resistance and plant growth period

The maximum root pullout resistance increased as a power function as plant growth periods increased (Fig. 3a). As plant growth periods increased from 4 to 7 a, the maximum root pullout resistance increased from 2.49 (±0.25) to 4.79 (±1.06) kN. Values of the maximum root pullout

resistance at different growth periods were not significantly different (P>0.05). The maximum root pullout resistance with a low increase rate of 13.86% for plants growth periods from 4 to 6 a, and a relatively high increase rate of 50.34% for plants growth periods from 6 to 7 a. As plant growth periods increased from 7 to 9 a, the maximum root pullout resistance increased from 4.79 (±1.06) to 7.20 (±2.38) kN with an increase rate of 48.00%. However, there was a significant difference in the maximum root pullout resistance between plant growth period of 9 a and those of 4, 5, and 6 a (P<0.05). As plant growth periods increased from 12 to 15 a, the maximum root pullout resistance increased from 12.84 (±4.45) to 14.71 (±4.96) kN with an increase rate of 5.06% (P>0.05). The maximum root pullout resistance for plant growth period of 12 a was significantly higher than that of 9 a, with an increase rate of 78.45%.

As shown in Figure 3b, the peak displacement of *C. korshinskii* roots increased linearly as growth periods increased. As growth periods extended from 4 to 15 a, the peak displacement of *C. korshinskii* roots increased from 11.77 (±8.61) to 26.50 (±16.09) cm. Difference between the peak displacement of the *C. korshinskii* roots at different growth periods was not significant (P>0.05).

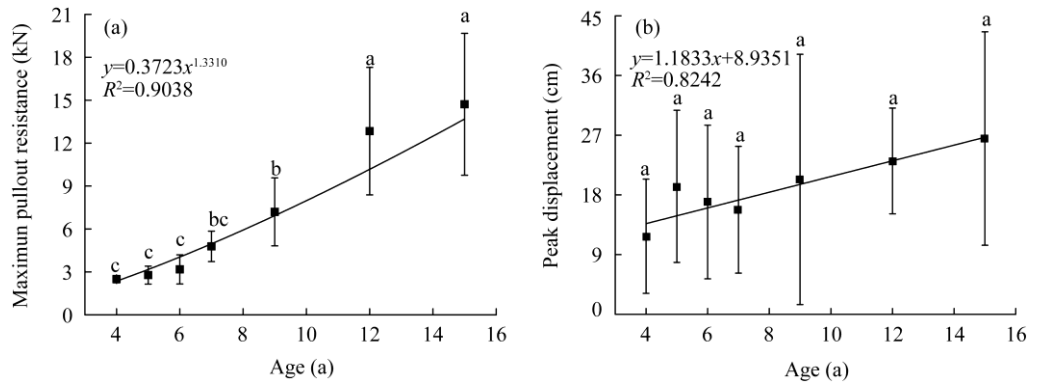

Fig. 3 Relationships of the maximum root pullout resistance (a) and peak displacement (b) with growth period of *C. korshinskii*. Different lowercase letters indicate significant different among different plant growth periods at P<0.05 level.

3.2 Relationships of root pullout resistance with plant height and plant crown breadth

As displayed in Figure 4, as plant height of *C. korshinskii* increased, the maximum root pullout resistance and peak displacement increased. However, the maximum root pullout resistance and peak displacement did not exhibit a significant functional relationship with plant height. And the correlation coefficients between these two indices and plant heights were 0.599 and 0.261, respectively.

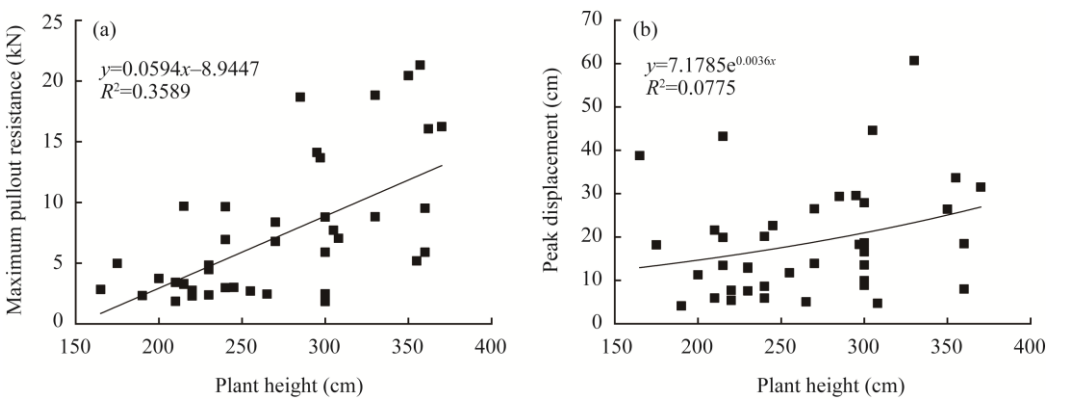

Fig. 4 Relationships of the maximum root pullout resistance (a) and peak displacement (b) with height of *C. korshinskii*

As illustrated in Figure 5a, the maximum root pullout resistance increased exponentially (R^2=0.5522) as plant crown breadth increased, but relationship between peak displacement and plant crown breadth was not significant (Fig. 5b). Correlation coefficients of the maximum root pullout resistance and peak displacement with plant crown breadth were 0.668 and 0.007, respectively. Thus, a moderate correlation between the maximum pullout resistance and plant crown breadth existed.

As plant height increased, plant crown breadth increased too (Fig. 6). There was no significant functional relationship between plant height and plant crown breadth. Correlation analysis demonstrated that correlation coefficient between plant height and plant crown breadth of *C. korshinskii* was 0.612.

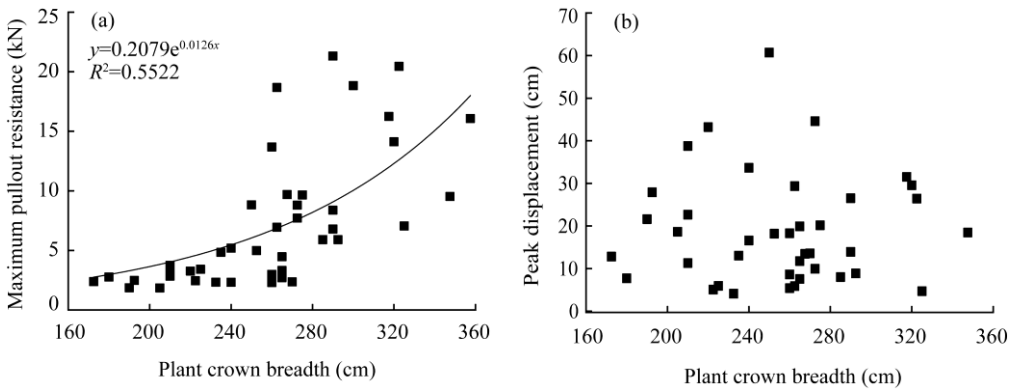

Fig. 5 Relationships of the maximum root pullout resistance (a) and peak displacement (b) with crown breath of *C. korshinskii*

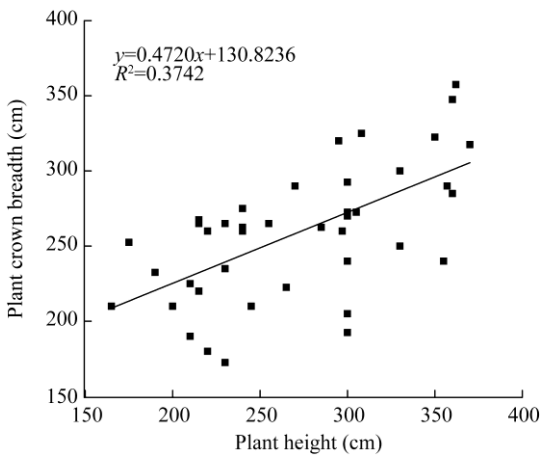

Fig. 6 Relationship between height and crown breadth of *C. korshinskii*

3.3 Characteristics of root pullout resistance, displacement curve, and root failure mode of *C. korshinskii*

Root pullout resistance and displacement curve of *C. korshinskii* obtained from *in situ* pullout test are shown in Figure 7. In this study, pullout resistance and displacement curve were divided into three stages: initial nonlinear growth stage (O–A), linear growth stage (A–B), and nonlinear stage (B–C) (Fig. 7a–c). In initial nonlinear growth stage, root pullout resistance increased nonlinearly as displacement increased, and the curve was concave. After initial nonlinear stage, the curve entered linear growth stage. In this stage, root pullout resistance increased nearly linearly with increasing displacement, and the curve was approximately a straight line. Linear growth stage terminated at point B, which was also the beginning of nonlinear stage (Fig. 7a–c). At nonlinear

stage, root pullout resistance reached the maximum value, after which root pullout resistance decreased as displacement increased. At nonlinear stage, the curve was jagged, and there were serval peaks.

Two modes of failure in a single root occurred when *C. korshinskii* roots were subjected to vertical loading forces (Fig. 7d). In the first mode, the periderm and the secondary vascular tissues of a single root were broken at the same time and at the same point (synchronous breakage mode), and the root diameter at the broken position was less than 12.55 mm. In the second mode, the periderm was broken first, and the secondary vascular tissue was pulled out along the periderm inner wall (periderm preferential breakage mode). Among 42 *C. korshinskii* plants, 57.14% and 11.43% of roots were broken in synchronous breakage mode and periderm preferential breakage mode, respectively, while 31.43% of broken roots combined these two modes. In this study, there was no test in which the roots were completely pulled out of the soil.

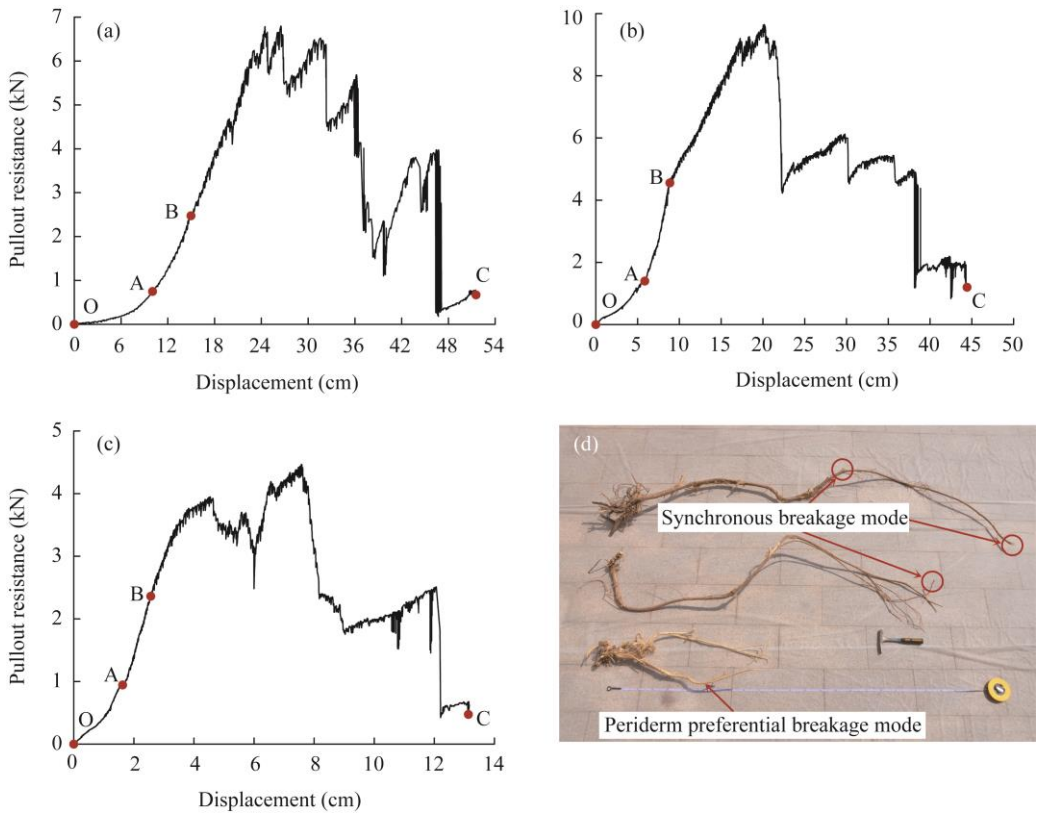

Fig. 7 Characteristics of pullout resistance and displacement curves of *C. korshinskii* (a–c), and typical failure modes of a single root of *C. korshinskii* (d). (a), Curve I; (b), Curve II; (c), Curve III.

4 Discussion

4.1 Variations of root pullout resistance and plant traits of *C. korshinskii*

In this study, the relationship of the maximum root pullout resistance and the peak displacement of *C. korshinskii* with plant growth periods was investigated. Results indicated that the maximum root pullout resistance increased as a power function (R^2=0.9038) with increasing growth periods. This was mainly related to root depth and lateral root number of *C. korshinskii*. Growth periods of *C. korshinskii* could be divided into young age (1–6 a), middle age (6–14 a), and old age (>14 a) (Cheng et al., 2005). Previous research has shown that root depth of *C. korshinskii* with a growth period of 2–4 a is 1.50–4.00 m (Niu et al., 2003). In the middle and old ages, root distribution depth can reach about 7.00–18.00 m (Hu, 1985; Cheng et al., 2005; Wang et al., 2015). In

addition, lateral root number of *C. korshinskii* with a growth period of 2–4 a is 8–39 (Niu et al., 2003). Therefore, root depth and lateral root number of *C. korshinskii* increased with increasing growth periods (Niu et al., 2003). The greater the root depth and lateral root number, the greater the interaction area and normal stress between root and soil, and the greater the maximum root pullout resistance (Stokes et al., 1996; Stokes et al., 2009; Ali et al., 2013).

Root peak displacement increased as a linear function (R^2=0.8242) with increasing plant growth periods. This is because longer growth periods lead to longer root lengths, increased tortuosity and higher lateral root numbers of *C. korshinskii*. Then, larger displacement is required to overcome the maximum root pullout resistance (Ennos, 1989; Mickovski et al., 2007; Schwarz et al., 2011). Owing to the randomness of root failure positions and the complexity of root architecture in *C. korshinskii*, the value range and discrete degree of root peak displacement of *C. korshinskii* were large at the same growth periods, resulting in no significant difference between root peak displacement and different growth periods (P>0.05).

Previous studies have shown that root traits have important effects on root pullout resistance (Dupuy et al., 2005; Stokes et al., 2009; Tian et al., 2014). However, if an empirical relationship between aboveground growth indices and root pullout resistance can be established, it will be convenient in assessing root pullout resistance in the field. In this study, results indicated that there was a moderate correlation between the maximum root pullout resistance and the height of *C. korshinskii* (r=0.599). This result was consistent with those of other plant species (Cucchi et al., 2004; Mickovski et al., 2005; Tanaka et al., 2011; Liu et al., 2013). In other words, the larger the plant, the higher its root pullout resistance (Liu et al., 2013). In addition, a moderate correlation between the maximum root pullout resistance and plant crown breadth (r=0.668) was obtained. By comparing correlation coefficient (r) and goodness of fit (R^2), we found that plant crown of *C. korshinskii* had a better correlation with root pullout resistance than plant height. Therefore, root pullout resistance of *C. korshinskii* can be estimated in the field by plant crown. In this study, a weak correlation was found between root peak displacement and its aboveground growth indices, which was related to the discrete degree of peak displacement data.

4.2 Mechanical process of uprooting of *C. korshinskii*

Characteristics of root pullout resistance and displacement curves reflect the root-soil interactions under external loading forces. Mechanics of uprooting involve processes that occurred in both root material and sediment matrix in which the root is located (Edmaier et al., 2014). In this study, root pullout resistance and displacement curve were divided into three stages: initial nonlinear growth, linear growth, and nonlinear stages. Initial nonlinear growth stage (Fig. 7a–c) occurred because tortuous roots that were closer to the source of vertical loading forces, needed to be straightened out when they were subjected to vertical loading forces (Commandeur and Pyles, 1991).

After initial nonlinear stage, the roots closest to the source of vertical loading forces underwent elastic deformation as vertical loading forces increased (Tian et al., 2014). Then, shear stress was induced at the root-soil interface (Ennos, 1989; Schwarz et al., 2010). At this time, root pullout resistance was determined by both root strength and shear strength of root-soil interactions. Within the range of elastic limit, the maximum shear stress at root-soil interface increased linearly as vertical loading forces increased (Schwarz et al., 2010). Consequently, at linear growth stage (Fig. 7a–c), root pullout resistance increased nearly linearly with increasing displacement (Tian et al., 2014). This stage also occurred in root pullout resistance and displacement curves of other studies, which were obtained via *in situ* pullout test with the roots of other plant species (Norris, 2005; Liu et al., 2013; Tian et al., 2014).

As vertical loading forces increased, once the shear stress at root-soil interface exceeded the elastic limit of root-soil interface or the soil around the root, root-soil interface entered the plastic deformation stage (Fig. 7a–c), resulting in plastic slip deformation (Schwarz et al., 2010; Tian et al., 2014). Plastic slip deformation zone extended along root-soil interface as load forces increased. At this stage, as plastic slip deformation zone expanded, elastic and shear stress zone at

root-soil interface, which was below plastic slip deformation zone, moved downward continuously along root surface, and the maximum shear stress in plastic slip deformation zone increased as load forces increased (Schwarz et al., 2010; Su et al., 2020). Thus, at this stage, root pullout resistance and displacement curve did not increase linearly any further. Theoretically, root pullout resistance should have increased nonlinearly until entire lower region of root-soil interface entered plastic deformation stage or breakage (Ennos, 1989). If root tensile strengths were greater than the maximum shear stress at each root-soil interface, root-soil interface of entire roots would enter plastic slip deformation state. Then, whole roots would separate from soil and slip out of ground (Norris, 2005; Schwarz et al., 2010). In contrast, taproot and lateral roots would break at the position with the weakest tensile strength along their lengths, resulting in root pullout resistance and displacement curve being jagged (Fig. 7a–c) (Bailey et al., 2002).

4.3 Failure modes of uprooting of *C. korshinskii*

Previous studies have shown that when roots are subjected to pullout force, failure mode of roots is mainly affected by factors including tensile strength of a single root, connection strength at the joints between mother and daughter branches, shear strength of root-soil interface, and root anatomical structure (Wu et al., 1979; Dupuy et al., 2005; Schwarz et al., 2010; Schwarz et al., 2011; Hu et al., 2013). When tensile stress in a single root (including joints between mother and daughter branches) is less than shear strength of root-soil interface and greater than tensile strength of a single root (or connection strength at the joints between mother and daughter branches), the root will fail at the position with the minimum tensile strength (Norris, 2005). In this study, *in situ* root pullout test showed that two modes of failure of a single root occurred when a *C. korshinskii* root was pulled out of the soil: synchronous breakage mode and periderm preferential breakage mode. Synchronous breakage mode was similar to those of previous studies (Norris, 2005; Rahardjo et al., 2014; Ji et al., 2016). However, few studies have reported periderm preferential breakage mode in other plant species.

Hu et al. (2013) studied root anatomical structure of *C. korshinskii* through microscopic observations, and found that *C. korshinskii* roots consisted of periderm, thin wall tissue of middle column sheath, and the secondary vascular tissue from outside to inside. The tensile strength of a single *C. korshinskii* root is mainly provided by periderm and the secondary vascular tissue (Hu et al., 2013). Mechanical properties of periderm and the secondary vascular tissue differ because of differences in their material composition. When a single root of *C. korshinskii* is subjected to tensile stress, periderm and the secondary vascular tissue may not break at the same time and position.

If periderm and the secondary vascular tissue of a single root are broken at a weak position at the same time, synchronous breakage mode has occurred. However, if periderm is broken first, it results in periderm preferential breakage mode. In this mode, shear strength of root-soil interface prevents periderm below breakpoint from being pulled out of soil, and shear strength of root-soil interface no longer plays a role in root pullout resistance. Thus, the secondary vascular tissue bears tensile stress by itself after periderm breakage, and it slips out along inner wall of periderm easily. This occurs because there is tissue fluid in the thin wall tissue of middle column sheath that can provide lubrication between periderm and the secondary vascular tissue. The secondary vascular tissue may break at the weakest position in its lower region later (Fig. 7d).

5 Conclusions

In this study, we found that the maximum root pullout resistance and the peak displacement increased as a power function and a linear function with the extension of plant growth periods, respectively. The maximum root pullout resistance increased exponentially with increasing plant crown breadth. Root pullout resistance and displacement curve were divided into three stages: an initial nonlinear growth stage, a linear growth stage, and a nonlinear stage. Synchronous breakage mode and periderm preferential breakage mode were found to be prevalent failure modes of

single roots during *C. korshinskii* uprooting. However, it was difficult to analyze the relationship between root pullout resistance and root characteristics, as well as the relationship between root characteristics and plant aboveground growth indices, because roots obtained through *in situ* pullout test were incomplete, and the characteristics of complete roots could not be measured. Moreover, there were unavoidable differences in plant site conditions in the field. Future studies should thus explore the characteristics of root pullout resistance via numerical simulation based on investigation of root distribution characteristics. The results of this study can serve as a theoretical foundation for further investigation of soil reinforcement and slope protection mechanisms of this shrub species in the loess area of northeastern Qinghai-Tibet Plateau, China. Furthermore, the dynamic changes in root characteristics of shrub species in the loess area of northeastern Qinghai-Tibet Plateau with the increasing plant growth periods will be the focus of future research.

Acknowledgements

This study was funded by the National Natural Science Foundation of China (42002283, 42062019), the Science and Technology Plan Project of Qinghai Province, China (2022-ZJ-Y08), and the Second Tibetan Plateau Scientific Expedition and Research (STEP) Program (2019QZKK0905, 2019QZKK0805). We thank all of the anonymous reviewers for providing helpful comments for the manuscript.

References

Ali F, Osman R, Kamil S S S M, et al. 2013. The influences of root branching patterns on pullout resistance. Electronic Journal of Geotechnical Engineering, 18: 3967–3977.

Bailey P H J, Currey J D, Fitter A H. 2002. The role of root system architecture and root hairs in promoting anchorage against uprooting forces in *Allium cepa* and root mutants of *Arabidopsis thaliana*. Journal of Experimental Botany, 53(367): 333–340.

Boldrin D, Leung A K, Bengough A G. 2017. Root biomechanical properties during establishment of woody perennials. Ecological Engineering, 109: 196–206.

Burylo M, Rey F, Roumet C, et al. 2009. Linking plant morphological traits to uprooting resistance in eroded marly lands (Southern Alps, France). Plant and Soil, 324: 31–42.

Cheng J M, Wan H E, Wang J, et al. 2005. Growth of *Caragana korshinskii* and depletion process of soil water in semi-arid region. Scientia Silvae Sinicae, 41(2): 37–41. (in Chinese)

Commandeur P R, Pyles M R. 1991. Modulus of elasticity and tensile strength of douglas-fir roots. Canadian Journal of Forest Research, 21(1): 48–52.

Crook M J, Ennos A R. 1996. The anchorage mechanics of deep rooted larch, *Larix europea*×*L. japonica*. Journal of Experimental Botany, 47(10): 1509–1517.

Cucchi V, Meredieu C, Stokes A, et al. 2004. Root anchorage of inner and edge trees in stands of Maritime pine (*Pinus pinaster* Ait.) growing in different podzolic soil conditions. Trees, 18(4): 460–466.

Dupuy L, Fourcaud T, Stokes A. 2005. A numerical investigation into the influence of soil type and root architecture on tree anchorage. Plant and Soil, 278(1–2): 119–134.

Edmaier K, Crouzy B, Ennos R, et al. 2014. Influence of root characteristics and soil variables on the uprooting mechanics of *Avena sativa* and Medicago sativa seedlings. Earth Surface Processes and Landforms, 39(10): 1354–1364.

Ennos A R. 1989. The mechanics of anchorage in seedlings of sunflower, *Helianthus annuus* L. New Phytologist, 113(2): 185–192.

Ennos A R. 1990. The anchorage of leek seedlings: the effect of root length and soil strength. Annals of Botany, 65(4): 409–416.

Fourcaud T, Ji J N, Zhang Z Q, et al. 2008. Understanding the impact of root morphology on overturning mechanisms: a modelling approach. Annals of Botany, 101(8): 1267–1280.

Genet M, Stokes A, Salin F, et al. 2005. The influence of cellulose content on tensile strength in tree roots. Plant and Soil, 278(1–2): 1–9.

Hu C L. 1985. Preliminary study on resistance physiology of several shrub species in arid and semi-arid areas of Qinghai Plateau. Science and Technology of Qinghai Agriculture and Forestry, (4): 24–31. (in Chinese)

Hu X S, Brierley G., Zhu H L, et al. 2013. An exploratory analysis of vegetation strategies to reduce shallow landslide activity

on loess hillslopes, Northeast Qinghai-Tibet Plateau, China. Journal of Mountain Science, 10(4): 668–686.

Ji X D, Chen L H, Zhang A. 2016. Anchorage properties at the interface between soil and roots with branches. Journal of Forestry Research, 28(1): 83–93.

Köstler J N, Bruckner E, Bibelriether H. 1968. The Roots of Forest Trees. Investigations of Root Morphology of Forest Trees in Central Europa. Hamburg: Verlag Paul Parey, 284. (in German)

Liu Y, Jia Z, Gu L, et al. 2013. Vertical and lateral uprooting resistance of *Salix matsudana* Koidz in a riparian area. Forestry Chronicle, 89(2): 162–168.

Liu Y B, Hu X S, Yu D M, et al. 2021. Influence of the roots of mixed-planting species on the shear strength of saline loess soil. Journal of Mountain Science, 18(3): 806–818.

Mickovski S B, Ennos A R. 2003. Anchorage and asymmetry in the root system of *Pinus peuce*. Silva Fennica, 37(2): 161–173.

Mickovski S B, Beek L, Salin F. 2005. Uprooting of vetiver uprooting resistance of vetiver grass (*Vetiveria zizanioides*). Plant and Soil, 278(1–2): 33–41.

Mickovski S B, Bengough A G, Bransby M F, et al. 2007. Material stiffness, branching pattern and soil matric potential affect the pullout resistance of model root systems. European Journal of Soil Science, 58(6): 1471–1481.

Norris J E. 2005. Root reinforcement by hawthorn and oak roots on a highway cut-slope in Southern England. Plant and Soil, 278(1–2): 43–53.

Niu X W, Ding Y C, Zhang Q, et al. 2003. Studies on the characteristics of *Caragana* root development and some relevant physiology. Acta Botanica Boreali-Occidentalia Sinica, 23(5): 860–865. (in Chinese)

Rahardjo H, Harnas F R, Indrawan I, et al. 2014. Understanding the stability of *Samanea saman* trees through tree pulling, analytical calculations and numerical models. Urban Forestry and Urban Greening, 13(2): 355–364.

Schwarz M, Cohen D, Or D. 2010. Root-soil mechanical interactions during pullout and failure of root bundles. Journal of Geophysical Research, 115: F04035, doi: 10.1029/2009JF001603.

Schwarz M, Cohen D, Or D. 2011. Pullout tests of root analogs and natural root bundles in soil: Experiments and modeling. Journal of Geophysical Research, 116: F02007, doi: 10.1029/2010JF001753.

Scippa G S, Michele M D, Iorio A D, et al. 2006. The response of *Spartium junceum* roots to slope: anchorage and gene factors. Annals of Botany, 97(5): 857–866.

Stokes A, Ball J, Fitter A H, et al. 1996. An experimental investigation of the resistance of model root systems to uprooting. Annals of Botany, 78(4): 415–421.

Stokes A, Atger C, Bengough A G, et al. 2009. Desirable plant root traits for protecting natural and engineered slopes against landslides. Plant and Soil, 324(1–2): 1–30.

Su L J, Hu B L, Xie Q J, et al. 2020. Experimental and theoretical study of mechanical properties of root-soil interface for slope protection. Journal of Mountain Science, 17(11): 2784–2795.

Stubbs C J, Cook D D, Niklas J K. 2019. A general review of the biomechanics of root anchorage. Journal of Experimental Botany, 70(14): 3439–3451.

Tan H B, Ma H Z, Zhang X Y, et al. 2006. Typical geochemical elements in loess deposit in the northeastern Tibetan Plateau and its paleoclimatic implication. Acta Geologica Sinica, 80(1): 110–117.

Tanaka N, Samarakoon M B, Yagisawa J. 2011. Effects of root architecture, physical tree characteristics, and soil shear strength on maximum resistive bending moment for overturning *Salix babylonica* and *Juglans ailanthifolia*. Landscape and Ecological Engineering, 8(1): 69–79.

Tian J, Cao B, Ji J N, et al. 2014. Biomechanical characteristics of root systems of *Hedysarum scoparium* and *Salix psammophila*. Transactions of the Chinese Society of Agricultural Engineering, 30(23): 192–198. (in Chinese)

van Beek L P H, Wint J, Cammeraat L H. 2005. Observation and simulation of root reinforcement on abandoned Mediterranean slopes. Plant and Soil, 278(1–2): 55–74.

Waldron L J, Dakessian S. 1981. Soil reinforcement by roots: calculation of increased soil shear resistance from root properties. Soil Science, 132(6): 427–435.

Wang G Y, Hu S H, Zhang Y J. 2017. An outdoor drawing test study of the root soil interaction force for a small tree root system. Hydrogeology and Engineering Geology, 44(6): 64–69. (in Chinese)

Wang X, Zhang J X, Lv W, et al. 2021. Infiltration response of deep dry soil to rainfall in the loess hilly region. Agricultural Research in the Arid Areas, 39(4): 29–38. (in Chinese)

Wang Y Q, Shao M A, Zhang C C, et al. 2015. Choosing an optimal land-use pattern for restoring eco-environments in a semiarid region of the Chinese Loess Plateau. Ecological Engineering, 74(74): 213–222.

Wu T H, Mckinnell W P, Swanston D N. 1979. Strength of tree roots and landslides on Prince of Wales Island, Alaska. Canadian Geotechnical Journal, 16(1): 19–33.

Xie L L, Sang Z G, He X H. 2013. SPSS Guide to Data analysis. Beijing: Posts & Telecom Press, 130. (in Chinese)

Yang M, D'ossez P, Danjon F, et al. 2017. Which root architectural elements contribute the best to anchorage of *Pinus* species? Insights from in silico experiments. Plant and Soil, 411(1–2): 275–291.

Yang M, D'ossez P, Danjon F, et al. 2018. Analyzing key factors of roots and soil contributing to tree anchorage of *Pinus* species. Trees, 32: 703–712.

Yang Q H, Zhang C B, Liu P C, et al. 2021. The role of root morphology and pulling direction in pullout resistance of alfalfa roots. Frontiers in Plant Science, 12: 580825, doi: 10.3389/fpls.2021.580825.

Zhang C B, Zhou X, Jiang J, et al. 2019. Root moisture content influence on root tensile tests of herbaceous plants. CATENA, 172: 140–147.

Zhang C B, Liu Y T, Liu P C, et al. 2020. Untangling the influence of soil moisture on root pullout property of alfafa plant. Journal of Arid Land, 12(4): 666–675.

Zhang X L, Hu X S, Li G R, et al. 2012. Time effect of young shrub roots on slope protection of loess area in Northeast Qinghai-Tibetan Plateau. Transactions of the Chinese Society of Agricultural Engineering, 28(4): 136–141. (in Chinese)

Zhou Y, Watts D, Li Y H, et al. 1998. A case study of effect of lateral roots of *Pinus yunnanensis* on shallow soil reinforcement. Forest Ecology and Management, 103(2–3): 107–120.

Zhuang J Q, Peng J B, Wang G H, et al. 2016. Prediction of rainfall–induced shallow landslides in the Loess Plateau, Yan'an, China, using the TRIGRS model. Earth Surface Processes and Landforms, 42(6): 915–927.